ELSEVIER

Computers and Chemical Engineering 25 (2001) 1185–1198

Computers & Chemical Engineering

www.elsevier.com/locate/compchemeng

An algorithm for evaluating reaction rates of catalytic reaction networks with strong diffusion limitations

Sergio P. Bressa [a,b], Néstor J. Mariani [a,b], Néstor O. Ardiaca [a,b], Germán D. Mazza [a,b], Osvaldo M. Martínez [a,b], Guillermo F. Barreto [a,b,*]

[a] *Departamento de Ingeniería Química, Facultad de Ingeniería, UNLP, 1900 La Plata, Argentina*

[b] *Centro de Investigación y Desarrollo en Procesos Catalíticos (CINDECA), UNLP, CONICET, C.C. 59, 1900 La Plata, Argentina*

Received 21 September 1999; received in revised form 16 February 2001; accepted 19 February 2001

Abstract

An *h*-adaptive mesh procedure to solve the reaction–diffusion problem for multiple reactions in catalytic pellets presenting strong diffusion limitations is developed. The discretization approach selected for this purpose is based on an integral formulation of the conservation equations. The adaptive mesh procedure relies on estimating the error of local reaction rate evaluations. By adding or removing nodes the errors will eventually become bounded within pre-set limits. The algorithm is tried on some test cases derived from the liquid phase catalytic hydrogenation of butadiene and butyne in butene (1, 2-*cis* and 2-*trans*) rich hydrocarbon mixtures.

Keywords: Catalytic reaction networks; Diffusion limitation; Numerical solution; Integral formulation; Adaptive procedure

Nomenclature

A	cross-section area (m^2)
Bi_k	Biot number of key-species k
C_k	molar concentration of species k (kmol m^{-3})
C_T	total molar concentration (kmol m^{-3})
D_k	effective diffusivity of species k (m^2 s^{-1})
$\mathbf{d}_i$	vector of residuals of Eqs. (11a), (11b) and (11c) (kmol m^{-3} s^{-1})
E_1	parameter for controlling precision in reaction rate evaluation
E_C	parameter for controlling convergence, Eq. (20)
$\mathbf{H}_i$	vector of variables defined in Eq. (17) (kmol m^{-3} s^{-1})
K	adsorption constant
L	length of catalyst slab (m)
N	number of subintervals
NGM	number of grid modifications
NI	number of iterations
NK	number of key species
$\underline{Q}_p$	$= D_p(C_p - C_{p,F})/L^2$; modified concentration for non-key species p (kmol m^{-3} s^{-1})
$\overline{R}$	average net consumption rate (kmol m^{-3} s^{-1})
r	reaction rate or net consumption rate (kmol m^{-3} s^{-1})
$\mathbf{U}_i$	vector of variables defined in Eq. (17) (kmol m^{-3} s^{-1})

* Corresponding author. Tel.: +54-221-4211353; fax: +54-221-4254277.
E-mail address: barreto@dalton.quimica.unlp.edu.ar (G.F. Barreto).

0098-1354/01/$ - see front matter
PII: S0098-1354(01)00694-9

x molar fraction
Y_k $= D_k(C_k - C_{k,F})/L^2$, modified concentration for key species k (kmol m^{-3} s^{-1})
z dimensionless coordinate inside the pellet

Greek letters
Φ Thiele modulus
σ matrix of stoichiometric coefficients
κ kinetic coefficient (s^{-1})

1. Introduction

Average reaction rates of catalytic reaction networks in pellets with diffusion limitations should be normally evaluated by employing a numerical procedure. Exceptions are linear kinetics and some specific networks and kinetics for which analytical approximations have been developed (Gonzo, Gottifredi and Romero, 1998; Gottifredi, Gonzo and Froment, 1994). The general case needing a numerical procedure is undertaken here.

Choosing an efficient numerical procedure to solve the reaction–diffusion problem can become critical, when simulating chemical reactors with the following features:

1. The diffusion limitation is strong and location of fast reaction zones inside the catalyst pellet can not be easily foreseen.
2. The number of stoichiometrically independent reactions is large.
3. The evaluation of the average reaction rates should be carried out many times to fulfil the objective of simulation.

Point (1) introduces the need of using a rather fine mesh for the discretization of the conservation equations.

Point (2) refers to the fact that reaction rate evaluations proportionally increase with the number of conservation equations (NK), and the operations to solve the linear systems resulting from a Newton-like method to conduct the iterative process increases as NK^3.

Regarding point (3), reactor simulation will introduce the need of evaluating average reaction rates in a number of spatial locations and/or time steps, sometimes in iterative way. If, additionally, the reactor operation should be simulated repeatedly, as for optimizing operating conditions (and/or design variables), average reaction rates will have to be evaluated many thousands (or higher orders) of times before reaching the final objective.

The three points operate as multiplication factors in defining the overall computational effort.

Another case involving optimization is when an intrinsic kinetic model should be developed from experimental data. Frequently, the experiments can be made with a catalyst sample ground into a particle size small enough to avoid transport effects. However, for dealing with non-uniform commercial catalysts, e.g., of the egg-shell type (Krishsna and Sie, 1994), grinding may not be practical. A reasonable alternative in these cases is to test the full size particles and analyse the data with a model introducing the diffusion effects.

A number of works dealing with the numerical solution of the reaction–diffusion problem for multiple catalytic reactions have been reported in the literature (Schilson and Amundson, 1961; Wohlfahrt and Hofmann, 1979; Wendt, Martinez, Lilley and Corley, 1979; Kaza and Jackson, 1980; Kaza, Villadsen and Jackson, 1980; Abashar and Elnashaie, 1993). Most of them have been employed for cases with moderate transport limitations. An exception is the work by Abashar and Elnashaie (1993) who studied methane reforming at conditions leading to very small effectiveness factors. They applied successfully a global orthogonal collocation method with collocation points shifted toward the pellet surface. This approach will be effective, when the fastest reactions take effectively place in a region close to the surface. However, when reactive species compete for adsorption sites, the fastest reactions can occur far from the pellet surface, if the more easily adsorbable species react less rapidly.

The aim of this paper is to present an algorithm to solve the reaction–diffusion problem by employing an automatic adaptive procedure for the grid of nodes at which reaction rates are evaluated. The algorithm has been conceived for multiple reactions and strong diffusion limitation, particularly when the location of fast reaction zones can not be easily foreseen.

The discretization approach selected for this purpose is based on the integral formulation of the conservation equations. The reasons for this choice will be given.

It is assumed in this contribution that Fick law can be used to describe the flow inside the catalyst. It will be outlined, however, how the algorithm can be extended to other more complex models of transport in porous media. It should be noted that no provision is made for the possible existence of multiple steady

states. As a consequence, a practical limitation for the use of the algorithm exists for conditions leading to multiplicity, either because of strong non-isothermal effects or because of the structure of some kinetic expressions (i.e. negative order reaction rates).

After presenting the different aspects of the proposed algorithm, some examples derived from the hydrogenation of unsaturated C_4 species on Pd catalysts will be employed as test cases.

2. Integral formulation

Consider NK key species reacting and diffusing within a pellet of length L. Assuming constant effective diffusivities $\{D_k\}_{k=1}^{NK}$, we define modified concentrations $Y_k = D_k(C_k - C_{k,F})/L^2$, where $\{C_k\}_{k=1}^{NK}$ are molar concentrations and the suffix F stands for values in the bulk fluid. The conservation equations can be written in vectorial notation as

$$\frac{d}{dz}\left(A(z)\frac{d\mathbf{Y}}{dz}\right) = A(z)\ \mathbf{r}, \tag{1}$$

where $\mathbf{Y} = [Y_k]_{k=1}^{NK}$, $\mathbf{r} = [r_k]_{k=1}^{NK}$ is the vector of net consumption rates and $A(z)$ is the cross-section area. Boundary conditions for Eq. (1) are assumed of the type

$$\frac{d\mathbf{Y}}{dz} = 0, \quad z = 0, \tag{2a}$$

$$\frac{d\mathbf{Y}}{dz} = -\mathrm{Bi}\mathbf{Y}, \quad z = 1, \tag{2b}$$

where Bi is the diagonal matrix of Biot numbers, $[\mathrm{Bi}_k]_{k=1}^{NK}$. Eq. (1) is integrated between $z = 0$ and a generic position $z = z'$, considering $\mathbf{r}$ as a non-homogeneous term $\mathbf{r}(z)$. Taking into account Eq. (2a), there results

$$\frac{d\mathbf{Y}}{dz'} = A(z')^{-1}\int_0^{z'} A(z)\,\mathbf{r}(z)\,dz. \tag{3}$$

Eq. (3) is now integrated from $z' = 0$ to $z' = z_i$. After expressing the resulting integral by parts,

$$\mathbf{Y}(z_i) - \mathbf{Y}(0) = P(z_i)\int_0^{z_i} A(z)\,\mathbf{r}(z)\,dz - \int_0^{z_i} P(z)A(z)\,\mathbf{r}(z)\,dz, \tag{4}$$

where,

$$P(z) = \int \frac{dz}{A(z)}. \tag{5}$$

For a catalyst slab, $A(z)$ is constant and $P(z)$ can be taken as $P(z) = z/A$. For cylindrical and spherical geometry $P(z)$ will be proportional to $\ln(z)$ and $(z)^{-1}$, respectively. The formulation is completed by considering Eq. (3) at $z' = 1$, along with the boundary condition Eq. (2b):

$$\left(\frac{dY}{dz}\right)\Big|_{z=1} = -\mathrm{Bi}\mathbf{Y}(1) = A(1)^{-1}\int_0^1 A(z)\mathbf{r}(z)dz. \tag{6}$$

Eqs. (4–6) can also be obtained from the Green function (Weinberger, 1967) for Eqs. (1), (2a) and (2b).

From now on, we will continue dealing specifically with a catalytic slab. Nonetheless, the treatment holds in every aspect for cylindrical or spherical geometry. Eq. (4) and Eq. (6) become for a slab

$$\mathbf{Y}(z_i) - \mathbf{Y}(0) = z_i\int_0^{z_i}\mathbf{r}(z)\,dz - \int_0^{z_i} z\,\mathbf{r}(z)\,dz, \tag{7a}$$

$$-\mathrm{Bi}\mathbf{Y}(1) = \int_0^1 \mathbf{r}(z)\,dz. \tag{7b}$$

3. Discretization of the integral formulation

The integrals in Eqs. (7a) and (7b) should be discretized for computational purposes. A possible way to do this is by defining trial functions for $\mathbf{Y}(z)$, from which $\mathbf{r} = \mathbf{r}(\mathbf{Y})$ can be integrated by a numerical procedure, in account of the general case considering non-linear rate expressions. Instead, we will employ trial function for $\mathbf{r}(z)$, as analytical evaluation of the integrals in Eqs. (7a) and (7b) is always possible, when conventional trial functions (i.e. polynomials) are chosen.

Given a set of nodes $\{z_i\}_{i=0}^{N}$ ($z_0 = 0$, $z_N = 1$), we consider the contribution to the integrals in Eqs. (7a) and (7b) of a generic subinterval (z_{j-1}, z_j). Local interpolating function for $r(z)$ of different degree can be formulated. The simplest approximation is a linear interpolating function on the subinterval end nodes z_{j-1}, z_j. Quadratic approximations can be obtained in at least two ways. One of them, termed here *Back Approximation*, interpolates between nodes z_{j-2}, z_{j-1} and z_j (the node previous to the subinterval is included), and the *Forward Approximation* uses z_{j-1}, z_j and z_{j+1} (the node next to the subinterval is included). Finally, the cubic approximation is based on the four mentioned nodes, z_{j-2}, z_{j-1}, z_j and z_{j+1}.

The formulation for the cubic approximation will be described next. The contributions

$$\mathbf{R}_j = \int_{z_{j-1}}^{z_j}\mathbf{r}(z)\,dz, \tag{8a}$$

$$\mathbf{W}_j = \int_{z_{j-1}}^{z_j} z\,\mathbf{r}(z)\,dz, \tag{8b}$$

can be expressed for $j = 2,\ldots, N-1$ as

$$\mathbf{R}_j = v_{j-2}^A\mathbf{r}_{j-2} + v_{j-1}^L\mathbf{r}_{j-1} + v_j^M\mathbf{r}_j + v_{j+1}^P\mathbf{r}_{j+1}, \tag{9a}$$

$$\mathbf{W}_j = w_{j-2}^A\,\mathbf{r}_{j-2} + w_{j-1}^L\mathbf{r}_{j-1} + w_j^M\,\mathbf{r}_j + w_{j+1}^P\mathbf{r}_{j+1}, \tag{9b}$$

where the weighting coefficients v_j^{α} and w_j^{α} arise from integrating the Lagrange interpolating polynomials on (z_{j-1}, z_j). The suffix j of $\mathbf{r}$ denotes evaluation at node z_j.

A special formulation should be employed for the first subinterval $(0, z_1)$ and for the last one (z_{N-1}, z_N). The former is constructed with the first three nodes plus the symmetry condition $d\mathbf{r}/dz = 0$ at $z = 0$, and the latter is constructed by interpolating on the nodes $z_{N-3}, z_{N-2}, z_{N-1}, z_N$. Thus,

$$\mathbf{R}_1 = v_0^L\mathbf{r}_0 + v_1^M\mathbf{r}_1 + v_2^P\mathbf{r}_2, \tag{10a}$$

$$\mathbf{W}_1 = w_0^L\mathbf{r}_0 + w_1^M\mathbf{r}_1 + w_2^P\mathbf{r}_2, \tag{10b}$$

$$\mathbf{R}_N = v_{N-3}^N\mathbf{r}_{N-3} + v_{N-2}^A\mathbf{r}_{N-2} + v_{N-1}^L\mathbf{r}_{N-1} + v_N^M\mathbf{r}_N, \tag{10c}$$

$$\mathbf{W}_N = w_{N-3}^N\mathbf{r}_{N-3} + w_{N-2}^A\mathbf{r}_{N-2} + w_{N-1}^L\mathbf{r}_{N-1} + w_N^M\mathbf{r}_N. \tag{10d}$$

With Eqs. (9a) and (9b) and Eqs. (10a), (10b), (10c) and (10d), we now write sequentially Eq. (7b) and Eq. (7a) for $i = N-1, N-2, \ldots, 1, N$:

$$\mathrm{Bi}\mathbf{Y}_N + v_{N-3}^N\mathbf{r}_{N-3} + \sum_{j=N-1}^{N} a_{N,j}\mathbf{r}_j + \sum_{j=0}^{N-2} A_j\mathbf{r}_j = 0, \tag{11a}$$

$$\mathbf{Y}_i - \mathbf{Y}_0 + \sum_{j=i-1}^{i+1}(b_{i,j} - z_i a_{i,j})\mathbf{r}_j + \sum_{j=0}^{i-1}(B_j - z_i A_j)\mathbf{r}_j = 0; \quad i = N-1, \ldots, 1, \tag{11b}$$

$$\mathbf{Y}_N - \mathbf{Y}_0 + (w_{N-3}^N - v_{N-3}^N)\mathbf{r}_{N-3} + \sum_{j=N-1}^{N}(b_{N,j} - a_{N,j})\mathbf{r}_j + \sum_{j=0}^{N-2}(B_j - A_j)\mathbf{r}_j = 0, \tag{11c}$$

where the weighting coefficients have been assembled into two groups. The values A_j and B_j gathered all contributions of a nodal value $\mathbf{r}_j$, except those of $\mathbf{r}_{N-3}$ for the last subinterval (v_{N-3}^N and w_{N-3}^N). For A_j,

$$A_j = v_j^A + v_j^L + v_j^M + v_j^P; \quad j = 0, \ldots, N-2, \tag{12a}$$

which is formally valid for all $j = 0, \ldots, N-2$ by assigning $v_0^M = v_0^P = v_1^P = 0$.

The remaining coefficients depend on each specific equation:

$$a_{i,i-1} = -v_{i-1}^A \quad (i = 1, \ldots, N-1);$$
$$a_{N,N-1} = v_{N-1}^L + v_{N-1}^M + v_{N-1}^P, \tag{12b}$$
$$a_{i,i} = v_i^M + v_i^P \quad (i = 1, \ldots, N); \quad a_{i,i+1} = v_{i+1}^P \quad (i = 1, \ldots, N-1). \tag{12c}$$

Similar definitions as those in Eqs. (12a), (12b) and (12c) hold for coefficients B_i, $b_{i,j}$ with respect to w_j^{α}.

The linear and quadratic approximations can be similarly formulated. In particular, for the Back Approximations, the formulation given above formally holds by dropping the weighting coefficients v_j^P, w_j^P, v_{N-3}^N, w_{N-3}^N.

4. Iterative solution by Newton method

A successive substitution scheme based on Eqs. (11a), (11b) and (11c) can be easily implemented by starting with trying nodal values $\mathbf{Y}_j^{\circ}$, evaluating $\mathbf{r}_j = \mathbf{r}(\mathbf{Y}_j^{\circ})$ and using Eqs. (11a), (11b) and (11c) in the sequence (a,c,b) to explicitly evaluate a new set $\mathbf{Y}_j$. Unfortunately, this procedure only converges for weak diffusion effects. Giona and Baratti (1993) carried out a numerical and functional analysis on this subject.

We will formulate here the Newton method to solve the equation set Eqs. (11a), (11b) and (11c). To do this, it should be recalled first that reaction rates would depend, in general, on the concentration of all reactants. Assuming that NP non-key species should be considered, and defining for them the vector of modified concentrations $\mathbf{Q} = [Q_p]_{p=1}^{\mathrm{NP}}$, $Q_p = D_p(C_p - C_{p,F})/L^2$, the reaction stoichiometry allows writing in vectorial notation for any position inside the pellet

$$\mathbf{Q} = \sigma\mathbf{Y} + \sigma^*\mathbf{Y}_N, \tag{13a}$$

where the nodal notation $\mathbf{Y}_N = \mathbf{Y}(1)$ is used, $\sigma = [\sigma_{p,k}]_{p,k=1}^{\mathrm{NP,NK}}$ is the matrix of stoichiometric coefficients and the coefficients of the matrix $\sigma^* = [\sigma_{p,k}^*]_{p,k=1}^{\mathrm{NP,NK}}$ are

$$\sigma_{p,k}^* = \sigma_{p,k}(\mathrm{Bi}_k/\mathrm{Bi}_p - 1). \tag{13b}$$

Temperature variations can also be accounted for by considering that one of the component of $\mathbf{Q}$, say Q_{NP}, is defined as $Q_{\mathrm{NP}} = \lambda_T(T - T_F)/L^2$, where λ_T is the effective thermal conductivity assumed as being a constant. The "stoichiometric coefficients" $\sigma_{\mathrm{NT},k}$ will be suitably defined heats of reaction.

Considering now the dependency $\mathbf{r} = \mathbf{r}(\mathbf{Y},\mathbf{Q})$, for Newton method, we should linearize each nodal value $\mathbf{r}_j$ around the trial value $\mathbf{Y}_j^{\circ}$, but according to Eq. (13a) also $\mathbf{Y}_N^{\circ}$ should be included. We will neglect here this last contribution, what will be valid for high Biot numbers ($\mathbf{Y}_N^{\circ} \to 0$) or when the ratios $\mathrm{Bi}_k/\mathrm{Bi}_p$ (Eq. (13b)) do not depart much from the unity. Cases in which this assumption can not be valid, particularly when dealing with thermal effects, will be discussed in the Appendix A.

Defining the matrix $\varphi = \partial\mathbf{r}/\partial\mathbf{Y} + (\partial\mathbf{r}/\partial\mathbf{Q})\sigma$, with the derivative matrices $\partial\mathbf{r}/\partial\mathbf{Y} = [\partial r_k/\partial Y_m]_{k,m=1}^{\mathrm{NK}}$ and $\partial\mathbf{r}/\partial\mathbf{Q} = [\partial r_k/\partial Q_p]_{k,p=1}^{\mathrm{NK,NP}}$, the linear expansion of $\mathbf{r}_j$ around $\mathbf{Y}_j^{\circ}$ is written,

$$\mathbf{r}_j = \mathbf{r}_j^{\circ} + \varphi_j\Delta\mathbf{Y}_j, \tag{14}$$

where $\Delta\mathbf{Y}_j = \mathbf{Y}_j - \mathbf{Y}_j^{\circ}$ are the Newton increments and both, $\mathbf{r}_j^{\circ}$ and φ_j, are evaluated at $\mathbf{Y}_j^{\circ}$ and, from Eq. (13a), $\mathbf{Q}_j^{\circ} = \sigma\mathbf{Y}_j^{\circ} + \sigma^*\mathbf{Y}_N^{\circ}$.

Once Eq. (14) is inserted in Eqs. (11a), (11b) and (11c), a linear set of equations arises for the increments $\Delta\mathbf{Y}_j$.

A simplification to improve the structure of the linear set of equations is made by avoiding the expansion of $\mathbf{r}_{i+1}$ in Eqs. (11b) and (11c) and that of $\mathbf{r}_{N-3}$ in the terms affected by v_{N-3}^{N} and w_{N-3}^{N} in Eq. (11a) and Eq. (11c) (i.e. taking $\mathbf{r}_{i+1}=\mathbf{r}_{i+1}^{\circ}$, $\mathbf{r}_{N-3}=\mathbf{r}_{N-3}^{\circ}$). As the contribution of an individual nodal value $\mathbf{r}_j$ to a given equation is relatively small (given the structure of the integral formulation, Eqs. (7a) and (7b)), it can be reasonably expected that this simplification will not bring any consequence on the stabilization of the iterative sequence. We found that this is effectively the case in practice. Only the increase of a unit in the number of iterations was occasionally noticed. The following set of equations arises,

$$\alpha_N\Delta\mathbf{Y}_N+\beta_N\Delta\mathbf{Y}_{N-1}+\mathbf{U}_{N-2}=-\mathbf{d}_N^{\circ}, \tag{15a}$$

$$i=N-1,\ldots,1$$

$$\begin{cases}\alpha_i\Delta\mathbf{Y}_i-z_i\mathbf{U}_{i-1}+\mathbf{H}_{i-1}+\beta_i\Delta\mathbf{Y}_{i-1}-\Delta\mathbf{Y}_0=-\mathbf{d}_i^{\circ};\\ \mathbf{U}_{i-1}-v_{i-1}\varphi_{i-1}\Delta\mathbf{Y}_{i-1}-\mathbf{U}_{i-2}=0;\\ \mathbf{H}_{i-1}-w_{i-1}\varphi_{i-1}\Delta\mathbf{Y}_{i-1}-\mathbf{H}_{i-2}=0;\end{cases} \tag{15b}$$

$$\alpha_0\Delta\mathbf{Y}_N+\beta_0\Delta\mathbf{Y}_{N-1}-\mathbf{U}_{N-2}+\mathbf{H}_{N-2}-\Delta\mathbf{Y}_0=-\mathbf{d}_0^{\circ}. \tag{15c}$$

In Eqs. (15a), (15b) and (15c) $\mathbf{d}_i^{\circ}$ are the residuals of Eqs. (11a), (11b) and (11c) evaluated with $\mathbf{Y}_j^{\circ}$. The matrices in Eqs. (15a), (15b) and (15c) are defined as:

$$\alpha_N=\mathrm{Bi}+a_{N,N}\varphi_N,\quad \beta_N=a_{N,N-1}\varphi_{N-1},$$
$$\alpha_i=\mathrm{I}+(b_{i,i}-z_i a_{i,i})\varphi_i,\quad \beta_i=(b_{i,i-1}-z_i a_{i,i-1})\varphi_{i-1}$$
$$(i=1,\ldots,N-1),\alpha_0=\mathrm{I}+(b_{N,N}-a_{N,N})\varphi_N,$$
$$\beta_0=(b_{N,N-1}-a_{N,N-1})\varphi_{N-1}, \tag{16}$$

where I denotes the identity matrix. The vector variables $\mathbf{U}_i$, $\mathbf{H}_i$ are defined by $\mathbf{U}_{-1}=0$, $\mathbf{H}_{-1}=0$,

$$\mathbf{U}_i=\sum_{j=0}^{i}A_j\varphi_j\Delta\mathbf{Y}_j;\quad \mathbf{H}_i=\sum_{j=0}^{i}B_j\varphi_j\Delta\mathbf{Y}_j\quad (i=0,\ldots,N-2), \tag{17}$$

as can be checked by applying recursively Eq. (15b). The variables $\mathbf{U}_i$, $\mathbf{H}_i$ are introduced in the system Eqs. (15a), (15b) and (15c) as additional unknowns to reduce the numerical cost of solving the linear set of equations. To appreciate this effect, Eqs. (15a), (15b) and (15c) can be written as

$$\mathbf{J}[\Delta\mathbf{Y}_N,\Delta\mathbf{Y}_{N-1},\mathbf{U}_{N-2},\mathbf{H}_{N-2},\Delta\mathbf{Y}_{N-2},\ldots,\mathbf{U}_0,\mathbf{H}_0,\Delta\mathbf{Y}_0]^{\mathrm{T}}$$
$$=-[\mathbf{d}_N^{\circ},\mathbf{d}_{N-1}^{\circ},\mathbf{0},\mathbf{0},\ldots,\mathbf{d}_0^{\circ}]^{\mathrm{T}}, \tag{18a}$$

where the structure of the Jacobian matrix J can be visualised in Eq. (18b), for $N=4$.

$$\mathbf{J}=\begin{array}{|cccccccccc|}
\multicolumn{10}{c}{\begin{array}{cccccccccc}\Delta\mathbf{Y}_4&\Delta\mathbf{Y}_3&\mathbf{U}_2&\mathbf{H}_2&\Delta\mathbf{Y}_2&\mathbf{U}_1&\mathbf{H}_1&\Delta\mathbf{Y}_1&\mathbf{U}_0&\mathbf{H}_0&\Delta\mathbf{Y}_0\end{array}}\\
\hline
\alpha_4&\beta_4&\mathrm{I}&0&&&&&&&0\\
&\alpha_3&-z_3\mathrm{I}&\mathrm{I}&\beta_3&&&&&&-\mathrm{I}\\
&&\mathrm{I}&0&-\mathrm{A}_2\varphi_2&-\mathrm{I}&&&&&0\\
&&&\mathrm{I}&-\mathrm{B}_2\varphi_2&0&-\mathrm{I}&&&&0\\
&&&&\alpha_2&-z_2\mathrm{I}&\mathrm{I}&\beta_2&&&-\mathrm{I}\\
&&&&&\mathrm{I}&0&-\mathrm{A}_1\varphi_1&-\mathrm{I}&&0\\
&&&&&&\mathrm{I}&-\mathrm{B}_1\varphi_1&0&-\mathrm{I}&0\\
&&&&&&&\alpha_1&-z_1\mathrm{I}&\mathrm{I}&\beta_1-\mathrm{I}\\
&&&&&&&&\mathrm{I}&0&-\mathrm{A}_0\varphi_0\\
&&&&&&&&&\mathrm{I}&-\mathrm{B}_0\varphi_0\\
\alpha_0&\beta_0&-\mathrm{I}&\mathrm{I}&&&&&&&-\mathrm{I}\\
\hline
\end{array} \tag{18b}$$

To transform J to an upper triangular matrix, the blocks $\{\alpha_i\}_{i=1}^{N}$ are first reduced and the left blocks in the bottom rows are eliminated afterwards. When performing these operations, the regular occurrence of identity matrices and null blocks should be properly considered. The number of multiplications (NMLS) for solving Eq. (18a) is proportional to N and the dominant term, regarding NK, is $(4N\times \mathrm{NK}^3)$, which indicates the strong effect of the reaction network size. When $\mathrm{NK}=1$, only the reduction of the last row of J should be carried out. The total NMLS and divisions to evaluate the unknowns in this case is exactly $(11N-5)$.

The addition of de $\mathbf{U}_i$, $\mathbf{H}_i$ as unknowns allows the banded structure of J (with the exception of the bottom block row and the rightmost block column). Instead, if $\mathbf{U}_i$, $\mathbf{H}_i$ are replaced in Eqs. (15a), (15b) and (15c) in terms of $\Delta\mathbf{Y}_j$ (from Eq. (17)) a matrix with blocks in every position above the main diagonal arises, which substantially increases the number of operations for solving the linear system in spite of the lower number of unknowns.

The application of Newton method for the linear and quadratic approximations leads to linear systems formally identical to that defined by Eqs. (15a), (15b) and (15c).

When $\mathrm{Bi}\to\infty$, $\mathbf{Y}_N=\mathbf{0}$, and Eq. (11a) and Eq. (15a) are eliminated from the previous formulation.

Two further details have been considered in implementing the Newton iterations.

When a fast irreversible reaction depletes a limiting species in a short distance from the catalyst surface, a coarser mesh can be employed for the rest of the particle, as arisen from the adaptive procedure described later. The nodal concentration of the almost extinguished species may follow a damped oscillatory pattern around zero for the coarse part of the grid, provided that the reaction rate gets negative values for negative concentrations of the limiting species. Many kinetic expressions do not satisfy this requirement, as kinetics of fractional order, which do not admit negative values. To avoid difficulties, the individual values $C_{k,j}$ are kept bounded by a low value (10^{-50} proved to be effective) if the value from the Newton method is negative. Other alternatives can also be convenient, as replacing factors of the type C^{γ} by $C\,|C|^{\gamma-1}$.

Far from the solution, the Newton method may produce too large increments. A step-length parameter $0 < \lambda < 1$ is then introduced to evaluate the new set of variables,

$$\mathbf{Y}_j = \mathbf{Y}_j^o + \lambda\ \Delta\mathbf{Y}_j. \tag{19}$$

The performance index $G_0 = \mathbf{d}_0\mathbf{d}_0^{\mathrm{T}}$ defined by the residual of Eq. (11c) is employed to evaluate λ. With $\mathbf{Y}_j$ calculated from Eq. (19), there results $G_0 = G_0(\lambda)$. The sequence $\lambda = (2/3)^n$ with $n = 0,1,\ldots, n_{\mathrm{MAX}}$ is tried and checked if $G_0(\lambda) < G_0(0)$. If this happens before $n = n_{\mathrm{MAX}}$, the current value of λ is adopted. If not, the value of λ defined with $n = n_{\mathrm{MAX}}$ is adopted and the iteration step finished. The value $n_{\mathrm{MAX}} = 2$ was always found adequate.

Alternatively, a more refined procedure based on the fact that the direction defined by the Newton increments is a descent direction for a performance index $G = \Sigma_{i=0}^{N}\mathbf{d}_i\mathbf{d}_i^{\mathrm{T}}$ can be employed to find the best λ by a line search (Press, Teukolsky, Vetterling and Flannery, 1992).

Finally, we recall the criterion employed to stop the Newton iterations. Convergence is assumed when for all indices k, j the difference between calculated and trial values satisfies

$$\left|Y_{k,j} - Y_{k,j}^{\circ}\right| \leqslant E_{\mathrm{C}}\, Y_{k,\max}, \tag{20}$$

where E_{C} is a given tolerance (i.e. in the range 10^{-5}–10^{-3}) and $Y_{k,\max}$ is the maximum nodal value.

5. Comparison with other numerical methods

Since the integral formulation has not been extensively employed in solving diffusion problems in catalysts, it is useful to make some remarks on the motivation for its choice as a basis for an h-adaptive mesh procedure (changing the position and number of nodes, while maintaining fixed the order of approximation).

The case of a single reaction and equidistant nodes will be considered here to analyse the basic properties of the different approximations presented in previous section and of other well known numerical methods.

A test condition is defined by a linear expression $r = \kappa C$, a Thiele modulus $\Phi = L(\kappa/D)^{0.5} = 10$, $\mathrm{Bi} \to \infty$ and a precision of 0.01% in estimating the average reaction rate $\overline{R} = \int_0^1 r\ \mathrm{d}z$. This level of precision will be satisfactory for most applications and it will be taken as a target level throughout this contribution.

The number of equally sized subintervals N needed by the three approximations described before (linear, quadratic and cubic) is given in Table 1. The number of reaction rate evaluations is $\mathrm{NRRE} = N + 1$. Also, the NMLS needed to solve the linear systems is given. A standard finite difference (FD) algorithm and two finite element methods (BEM1D, SOC), which will be defined below, are also included.

The linear approximation is definitely inefficient as judged by the needed value of N. Neither the quadratic Back Approximation seems to be justified in comparison with the cubic one. However, the quadratic approximations will be useful in the adaptive mesh procedure described later on.

The FD method requires the same number of nodes as the linear approximation. A lower value of NMLS results, however, as the triangular matrix in this case only demands $\mathrm{NMLS} = 4N$ multiplications.

The numerical method indicated as BEM1D is the code presented by Ramachandran (1994). It also employs an integral formulation, but on an element basis. Each end-point of an element provides concentration and its derivative as unknowns. A third-degree osculating polynomial (i.e. an approximation with cubic Hermite polynomials as shape functions) is used for the local concentration profile, from which integral contributions (those defined by Eqs. (8a) and (8b)) are evaluated by Gauss–Legendre quadrature for non-linear kinetics. Although the code BEM1D employs 10-point quadrature, it is most probably that 3 or 4 quadrature points will suffice in most cases. The number of reaction rate evaluations given in Table 1 corresponds to 3 quadrature points ($\mathrm{NRRE} = 3\mathrm{NE}$).

In BEM1D, the jacobian matrix J for the Newton increments has a pentadiagonal structure, demanding for its solution $\mathrm{NMLS} = 14 \times \mathrm{NE} - 2$.

SOC in Table 1 is Spline Orthogonal Collocation (Villadsen and Michelsen, 1978), which is also known as Orthogonal Collocation on finite elements. A local cubic approximation for C requiring two internal collocation points per element ($\mathrm{NRRE} = 2 \times \mathrm{NE}$) was used. As regards the linear system for Newton method, cubic

Table 1
Number of subintervals (N) or elements (NE), reaction rate evaluations (NRRE), and multiplications for solving linear systems (NMLS) demanded by different methods to reach a precision of 0.01% in evaluating $\overline{R}$ for linear kinetics ($\Phi = 10$)

Method	Linear	Quadratic (Back)	Cubic	FD	BEM1D	SOC
N (or NE)	200	55	22	200	16 (NE)	19 (NE)
NRRE	201	56	23	200	48	38
NMLS	1800	600	237	800	222	264

SOC using Hermite polynomial as shape functions leads to the same structure as BEM1D (NMLS = 14 × NE − 2).

By comparing the cubic approximation presented above with the other two cubic finite element method (BEM1D, SOC), it can be appreciated that the former saves a considerable amount of reaction rate evaluations. This fact can be explained as follows. If a subinterval (z_{j-1}, z_j) is assimilated to an element, the present cubic approximation is built from the values at the ends of the element and at the two adjacent nodes, thus conforming a set of overlapping polynomials. Instead, the finite element methods BEM1D and SOC use a cubic approximation locally built from values and first derivatives at the ends of each element. This kind of approximation is expected to be more accurate, but needs doubling the number of unknowns. As an overall result, BEM1D and SOC effectively need slightly fewer elements, but more reaction rate evaluations.

The values of NMLS for the three cubic methods do not show significant differences between them. However, assuming that the values of N and NE remain the same for a given multiple reaction problem (NK reactions), NMLS will change with respect to the single reaction case. Thus, for the present cubic approximation the highest order term (NK^3) of NMLS is $(4N)NK^3$, while for BEM1D and SOC it is $(8 \times NE)NK^3$. From the values of N and NE in Table 1, we can appreciate that the cubic integral formulation will save a significant number of operations for a value of NK higher than 3 or 4, from which NMLS starts to be neatly dominated by the term in NK^3.

The results for other kinetic expressions show an increasing trend of N (or NE) with the order of reaction γ ($r = \kappa C^{\gamma}$). For instance, at $\Phi = L\sqrt{\kappa(\gamma+1)C_F^{\gamma-1}/(2D)} = 10$, the values for $\gamma = (0.5, 1, 2)$ are NRRE = (12, 23, 33) for the cubic approximation and NRRE = (28, 38, 48) for SOC. Although, the order γ introduces variations of some relevance, the parameter Φ is more significant, as shown next.

The results in Table 1 can be extended to higher values of Φ. Assuming that Φ is large enough for the reactive species being depleted inside the catalyst, the penetration depth X will decrease as Φ^{-1} (Villadsen and Michelsen, 1978, Chapter 7). For most types of rate expressions, and particularly for a first-order reaction, these conditions will already be reached for $\Phi = 10$. Then, we can write, $X = X_{10}(10/\Phi)$. As the behaviour of any method employing local approximations will depend on how many elements or nodes fall within X, the values of N or NE needed to reach a given precision will increase as Φ does. Then,

$$N = N_{10}\left(\frac{\Phi}{10}\right); \quad \mathrm{NE} = \mathrm{NE}_{10}\left(\frac{\Phi}{10}\right). \tag{21}$$

For example, the actual value of NE for SOC at $\Phi = 100$ is NE = 185, and Eq. (21) predicts NE = 190. Eq. (21) clearly shows the impact on the number of nodes or elements introduced by the diffusion limitations. It will also be valid for multiple reactions on the basis of a properly defined Thiele modulus. Even though the same value of N or NE may be needed by a single or a multiple reaction system, the numerical cost in the last case will depend on the number of reactions NK for evaluating the reaction rates, on NK^2 for their derivatives and on NK^3 for solving the linearized systems.

Although the case of a single reaction has been useful to illustrate the essential features of the reaction–diffusion problem and the behaviour of numerical procedures, specific strategies can be applied to deal with a single reaction under strong diffusion limitations, as the penetration depth can be estimated in advance (Villadsen and Michelsen, 1978, Chapter 7). Instead, an adaptive procedure will be justified for multiple reactions, as it will allow simultaneously locating the zone (or zones) of fast reaction rates, refining the mesh within those zones and finding the solution of the conservation balances.

Higher order finite element formulations have not been considered here. Although they can be convenient if a high level of precision is required, a drawback can be anticipated when using an h-adaptive mesh procedure (i.e. leaving fixed the order of approximation and modifying the number and distribution of nodes) as proposed below. As a high order of approximation involves a large number of unknowns, adding an element may introduce more degrees of freedom than needed, while removing an element may drop the precision below the tolerance. Among the different methods discussed above, the present formulation and FDs are optimal in this context, as only one degree of freedom is involved, when a node is removed or added. The other cubic approximations discussed above involve two degrees of freedom per element.

From the above given discussion, it can be concluded that the formulation here proposed is an adequate alternative for building an h-adaptive mesh algorithm. Nonetheless, the convenience of the present formulation as a general purpose method should not be over-emphasized, as the following limitations are worth noting:

(a) The approximation order can not be raised above three in a way as simple as for other methods. Also, the treatment for the end subintervals will become highly asymmetric with respect to the interior elements.

(b) For relatively mild diffusion effects (tentatively defined by $\Phi < 10$), the method will not be usually as efficient as global methods, such as global the orthogonal collocation.

(c) The use of the method can not be directly extended for non-linear mass transport models. Although it may be employed for some cases (as briefly commented on at the end of Section 8), an auxiliary set of equations is needed.

(d) There is not a direct way to extend the use of the approximating polynomials in one-dimensional problems to two or three-dimensional cases. The integral formulation in these cases becomes the basis for Boundary Element Methods, for which radial basis functions are conveniently employed to approximate non-linear terms (Golberg, Chen and Bowman, 1999).

(e) Due to point (a), the method can not be recommended for a p or h–p adaptive strategy.

6. Adaptive mesh procedure

Given an initial node distribution, the procedure proposed to add or remove nodes is described here.

The calculations are first carried out using the quadratic Back Approximation described before. After obtaining convergence with the current grid distribution, the error in evaluating each value $R_{k,j}$ (Eqs. (8a) and (8b)) is estimated. With the available nodal values $r_{k,j}$, the contributions $R^*_{k,j}$ resulting from using the formulation of the quadratic Forward Approximation (note that equations are not solved with this approximation) are calculated. The difference $\Delta_{k,j} = |R_{k,j} - R^*_{k,j}|$ is a measure of how much the local profile of r_k departs from a quadratic function. If with a suitable grid this difference can be maintained low enough everywhere, it can be assumed that the difference is dominated by the missing cubic term in the local approximation of r_k. Once this situation is reached, the last grid is expected to be suitable for using the cubic approximation as the final stage in the algorithm.

The significance of the differences $\Delta_{k,j}$ will be assessed with respect to the reference magnitude $R_{A,k}$ defined as

$$R_{A,k} = \frac{1}{2}\sum_{j=1}^{N}(|R_{k,j}| + R_{k,j}), \tag{22}$$

$R_{A,k}$ is used instead of the average net consumption rate $\overline{R}_k$,

$$\overline{R}_k = \sum_{j=1}^{N} R_{k,j}, \tag{23}$$

because $\overline{R}_k$ may be nearly nil for species being produced in some regions of the catalyst and consumed in others.

For each subinterval (z_{j-1}, z_j), $j = 1,\ldots, N$, the ratios $\{\Delta_{k,j}/R_{A,k}\}_{k=1}^{NK}$ are compared to three control parameters E_0, E_1 and E_2. An adaptive decision is made by applying sequentially, from $j = N$ (pellet surface) to $j = 1$, the following criteria:

- if for any k, $(\Delta_{k,j}/R_{A,k}) \geqslant E_2$, two equidistant nodes are added in the subinterval $(z_{j\text{-}1}, z_j)$. If not,
- if for any k, $E_1 \leqslant (\Delta_{k,j}/R_{A,k}) < E_2$, one node is added in the middle of (z_{j-1}, z_j). If not,
- if for all k, $(\Delta_{k,j}/R_{A,k})$ and $(\Delta_{k,j-1}/R_{A,k}) < E_0$, and node z_{j+1} was maintained, node z_j is removed. If not,
- no modification is made in the subinterval (z_{j-1}, z_j).

Parameters E_0 and E_2 can be written as $E_0 = E_1/\mathrm{B0}$, $E_2 = E_1 \times \mathrm{B2}$. The values of B0 and B2 should not be too low, as an oscillatory behaviour may arise in the course of the stages, eliminating certain nodes in a given stage and adding them in the next. A minimum value of 10 is suggested for both.

Instead of iterating until condition (Eq. (20)) is satisfied, the grid modification is tried just when,

$$|Y_{k,j} - Y^{\circ}_{k,j}| \leqslant E_C \times \mathrm{BC} \times \mathbf{Y}_{k,\max}, \tag{24}$$

where BC is a parameter higher than one. It is assumed that the precision level defined by ($E_C \times$ BC) is enough to apply the grid adaptive procedure. The product ($E_C \times$ BC) should not result much higher than E_1, as the oscillating behaviour described above may also occur even for suitable values of B0 and B2.

The value of E_C should be also suitably related to E_1 to guarantee that the precision defined by the latter is effectively obtained without making wasteful iterations. In practice, E_C should be taken about one order of magnitude below E_1, but values lower than two orders will probably lead to useless iterations.

In summary, the five parameters E_C, BC, E_1, B0 and B2 control the precision of Newton iterations, the error in estimating $\overline{R}_k$ and the course of the adaptive procedure. For the examples described in this and next sections, the following values were adopted: $E_C = 2 \times 10^{-4}$, $\mathrm{BC} = 50$, $E_1 = 5 \times 10^{-3}$, $\mathrm{B0} = 20$ and $\mathrm{B2} = 20$.

The adaptive strategy outlined above relies upon the size of the subinterval (z_{j-1}, z_j) to determine the precision of $R_{k,j}$. Although this is of primary importance, the actual precision will depend secondarily on the size of the adjacent subintervals. It is then a good practice to avoid the ratio between the size of adjacent subintervals being larger than a pre-set value. This feature can be readily added to the above given adaptive strategy. Thus, as an additional condition to remove a node, the maintenance of the size ratio below the pre-set value should be checked. Also, when the criteria given above indicate that nodes are to be inserted, the new set of size ratios is checked and additional nodes are added in some subintervals so that the size ratios can satisfy the tolerance. A value of 4 is suggested as the maximum size ratio. This feature was proved to be of some significance for very large diffusion resistances (in terms of Thiele modulus, $\Phi > 100$).

Once a given stage during the adaptive procedure reveals that no node should be added, the grid is adopted as definitive and the cubic approximation is applied along with Newton method until condition (Eq. (20)) is reached.

A remark concerns the evaluation of $\mathbf{R}^*_N$, as the Forward Approximation would require a node at the right of the subinterval (z_{N-1}, z_N). Instead, the derivative $(\mathrm{d}\mathbf{r}/\mathrm{d}z)|_{z=1}$ is employed, which is evaluated with

Table 2
Comparison between values of subintervals needed by adaptive and uniform grid procedures, for a single first-order reaction

Φ	10	20	50	100	200	500	1000
N (uniform)	22	44	110	220	440	1100	2200
N (adaptive)	11	14	13	14	17	17	17

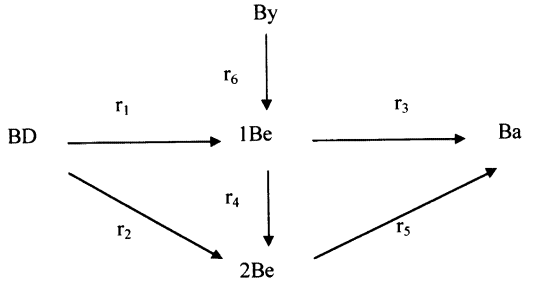

Fig. 1. Scheme of reaction network.

the aid of Eq. (6) as $(\mathrm{d}\mathbf{r}/\mathrm{d}z)\big|_{z=1} = \varphi_N \overline{\mathbf{R}}$, where the derivative matrix φ_N and $\overline{\mathbf{R}}$ result from the values calculated using the Back Approximation. Then, $\mathbf{R}_N^*$ is evaluated from the quadratic expression which satisfies $\mathbf{r}_{N-1}$, $\mathbf{r}_N$ and $(\mathrm{d}\mathbf{r}/\mathrm{d}z)\big|_{z=1}$.

To gain a first impression on the effect of the adaptive procedure, we consider again the case of a single first-order reaction. The number of subintervals N using both, a uniform grid and the adaptive procedure, is shown in Table 2 for different values of the Thiele modulus Φ. The values of N corresponding to uniform grids are calculated from Eq. (21) and $N_{10} = 22$ for the cubic approximation (Table 1). The precision obtained for $\overline{R}$ with the adaptive procedure is, on average, 1.7×10^{-4}. Therefore, the results are comparable to those when a uniform grid is employed. The initial grid was $\{z_i\}_{i=0}^{i=7} = (0, 0.5, 0.7, 0.8, 0.9, 0.97, 0.99, 1)$ and the final configuration was reached after two or three modification stages.

The adaptive procedure distributes nearly the same amount of nodes within the penetration length, irrespective of the value of Φ. The moderate increasing trend for the values of N as Φ rises is mainly due to the effect of keeping a maximum ratio between adjacent subinterval sizes.

When the additional effort for the grid modification stages is taken into account, we can expect that the use of the adaptive procedure will start to be justified for Φ larger than 10–20. For a general case involving multiple non-linear reactions, there will be always a value of Φ from which an adaptive procedure will be advantageous over solving the problem with a fixed node distribution. It is worth remarking that the control error parameter was $E_1 = 5 \times 10^{-3}$, but the error in evaluating $\overline{R}$ is significantly smaller (1.7×10^{-4}). In general, the precision reached is at least one order of magnitude higher than that indicated by E_1, mainly because the cubic approximation is used to obtain the final results after the grid is found suitable with a quadratic approximation.

7. Test examples

The algorithm presented above is employed in this section for some examples derived from the catalytic hydrogenation of unsaturated C_4 species in liquid phase. One of the main practical purposes of this process is to hydrogenate selectively small amounts of acetylenic compounds (1-butyne, By, is considered here) and dienes (typically 1-3 butadiene, BD) in C_4 cuts rich in olefins, 1-butene (1Be), *cis*-2-butene and *trans*-2-butene. Isobutene may also be present in streams of commercial interest, but it has practically no reactivity. Some important features of this system will be summarized below. Further discussion on the subject is undertaken by Bressa, Ardiaca, Martinez, and Barreto (1998).

Commercial catalysts contain Pd as the main catalytic agent impregnated on a thin external layer of the order of 100 μm (egg-shell catalyst). A simplified scheme of the reaction network at 300–340 K is presented in Fig. 1, where 2Be represents a lump of *cis*- and *trans*-2-butenes and Ba represents *n*-butane. For simplicity, the isomerization of 1Be to the 2Be lump is considered as being irreversible as 2-butenes are thermodynamically favoured.

The reaction rate expressions can be expressed as (Bressa et al., 1998)

$$r_i = C_{\mathrm{T}} \frac{\kappa_i K_k x_k x_{\mathrm{H_2}}}{\Lambda}, \tag{25a}$$

$$\Lambda = K_0 + \sum_{k=1}^{\mathrm{NK}} K_k x_k, \tag{25b}$$

where C_{T} is the overall molar concentration, x_k is the molar fraction of the unsaturated species reacting in the ith reaction (Fig. 1), NK corresponds to the number of unsaturated species and K_0 accounts for adsorption of saturated species. The value of K_0 is small enough to ensure that unsaturated species will normally cover all catalytic sites.

The system is characterized by very large differences between the adsorption constants K_k, in the sequence By ≫ BD ≫ 1Be > 2Be. If By is present in the system, BD will only start to react when By has been almost depleted. In turn, BD should react up to reach a very small concentration for reactions of 1Be and 2Be to become noticeable. In the presence of strong diffusion resistance inside the pellet, the reactants will be consumed consecutively from the pellet surface.

According to kinetic expressions (Eqs. (25a) and (25b)), when a given species saturates the catalytic sites, it reacts following a zero-order regime at a rate ($C_{\mathrm{T}}\ \kappa_k\ x_{\mathrm{H2}}$), where κ_k is the sum of all kinetic coefficients for

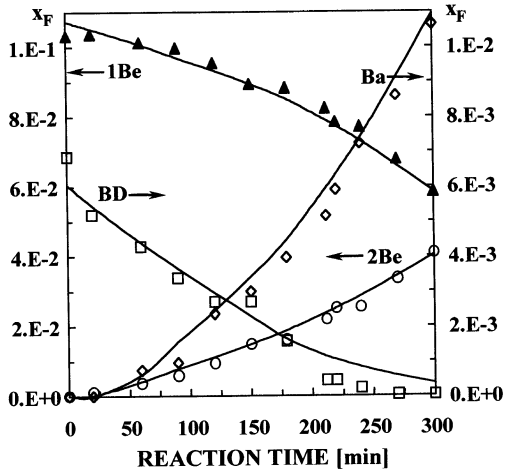

Fig. 2. Comparison between experimental data and model.

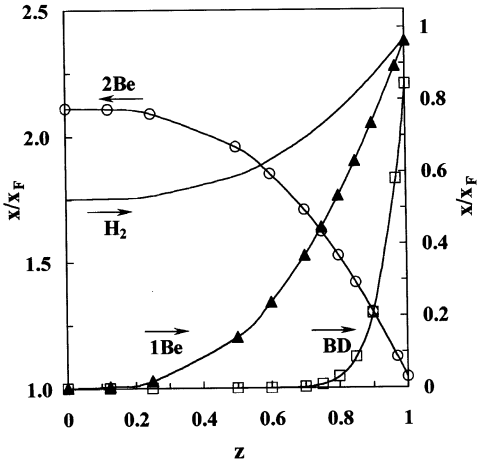

Fig. 3. Profiles for Case I (Table 2).

that species. The values κ_k usually follow the reverse trend of adsorption constants. This makes it possible that the fastest reactions can take place well inside the pellet and not close to the surface. In this sense, By is definitely slower than the other unsaturated species. Case III defined below is intended to show this effect.

The existence of strong diffusion limitation within the thin active layer of these commercial catalysts is due to the intrinsically slow diffusion in liquid phase and the fact that Pd is a very active catalytic agent for the hydrogenation of unsaturated hydrocarbons. Although the activity can be moderated by the content of Pd (usually around 0.1%), these catalysts are known to become deactivated by deposition of heavy residues (green oil) (Boitiaux, Cosyns, Derrien and Leger, 1985). Hence, a lower initial activity (using less Pd content) will surely shorten the time of the catalyst under continuous service without regeneration or replacing. A daily loss of 1% in activity would lead after two years to about one thousand of the initial catalyst activity. For an analysis of the global strategy in catalyst design, the presence of By should be particularly considered. By is adsorbed much more strongly than any of the other unsaturated species but it reacts at a considerably slower rate (self-inhibition). Therefore, the activity level will be important to avoid very large catalyst loading.

Experimental results obtained in a batch laboratory reactor with a commercial catalyst have been presented by Bressa et al. (1998) at constant temperature and pressure (40°C and 8 atm). By was not present in the experimental mixture. The results of a regression analysis of data plotted in Fig. 2 using the kinetic model given by Eqs. (25a) and (25b) are presented here. The values employed for transport parameters are given in Table 3. The length of the catalytically active shell was $L = 100$ μm.

Estimated values of kinetic parameters from regression are also given in Table 3 (Case I and common data). The structure of the kinetic model (Eqs. (25a) and (25b)) needs one parameter to be fixed arbitrarily ($K_{1Be} = 1$ was chosen). Values of kinetic and adsorption coefficients for the 2Be lump (κ_5 and K_{2Be}) and K_0 could not be evaluated with statistical significance as the reaction time was not long enough to allow an identification of 2Be hydrogenation. Therefore, the values of κ_5, K_{2Be} and K_0 in Table 3 are just mathematically suitable. A good match between experimental and adjusted model values is achieved, as it is shown in Fig. 2.

Molar fractions in the bulk liquid defined for Case I in Table 3 correspond to the end of the experiment. The estimated profiles inside the pellet are displayed in Fig. 3. The effectiveness factor (average reaction rate relative to reaction rate at bulk composition) for BD is about 1/10 and the Thiele modulus $\Phi_{BD} = L\sqrt{r_{BD,F}/(C_T x_{BD,F} D_{HC})} = 9.5$. The effectiveness factor for the net consumption of 1Be is larger than one (about 1.6), because its reactions become enhanced inside the pellet due to BD depletion.

Table 3
Values of parameters employed in Figs. 2–5[a]

Case	$x_{BD,F}$	$x_{1Be,F}$	$x_{2Be,F}$	$x_{H2,F}$	$\kappa_{BD} = \kappa_1 + \kappa_2$	$\kappa_{1Be} = \kappa_3 + \kappa_4$	$\kappa_{2Be} = \kappa_5$	K_{BD}
I	0.00037	0.0584	0.040	0.008	0.47	3.3	0	416
II	0.00050	0.0600	0.040	0.030	4.0	30	30	500
III	0.00800	0.0600	0.040	0.030	0.2	100	30	10000

[a] Common data: $D_{H2} = 0.321 \times 10^{-8}$ m^2 s^{-1}, $D_{HC} = 0.082 \times 10^{-8}$ m^2 s^{-1}, $Bi_{H2} = 39.5$, $Bi_{HC} = 63.2$, $C_T = 7$ kmol m^{-3}, $(\kappa_2/\kappa_1) = 9$, $(\kappa_4/\kappa_3) = 2.3$, $K_{1Be} = 1$, $K_{2Be} = 0.01$, $K_0 = 1 \times 10^{-5}$, $[\kappa_i] = s^{-1}$.

An initial grid and initial guess values x_k^o to start the iterative and adaptive procedure should be provided. For this and the other cases analyzed below, the initial grid was $\{z_i\}_{i=0}^{i=7} = (0, 0.5, 0.7, 0.8, 0.9, 0.97, 0.99, 1)$. The initial set $\{x_{k,i}^o\}_{i=0}^{i=7}$ was obtained by transforming the reaction rates to linear expressions. To this end, the inhibition term Λ and x_{H2} in Eqs. (25a) and (25b) were evaluated with the bulk composition and left fixed inside the catalyst. Therefore, each kinetic expression thus obtained depends linearly on the molar fraction of the corresponding unsaturated species. This problem is straightforwardly solved for the initial grid, and the values x_k^o so obtained are employed to start the simultaneous iterative and adaptive procedure described in Section 6. The number of subintervals, iterations and reaction rate evaluations are given for this and other cases in Table 3, along with values obtained by using equidistant nodes. A comparison between the adaptive procedure and the use of equidistant nodes will be undertaken at the end of this section.

The final results for Case I were reached in NI = 10 iterations and the number of subintervals was $N = 11$ (75% between the surface and the middle of the active layer). The adaptive process demanded NGM = 2 grid modifications.

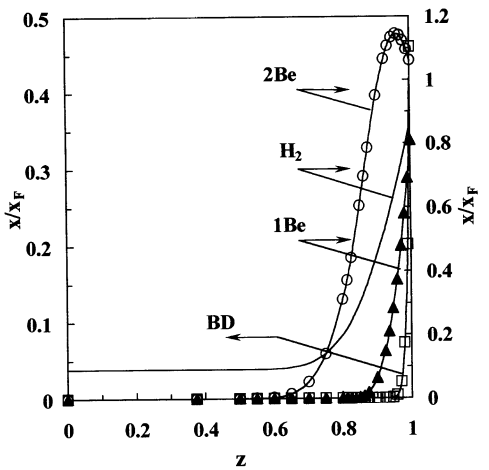

Fig. 4. Profiles for Case II (Table 2).

Table 4
Number of subintervals N, grid modifications NGM, iterations NI and evaluations of the reaction rate set $\mathrm{NRRE} = \Sigma_n(1+N_n)\mathrm{NI}_n$ for solving the cases defined in Table 3 with the adaptive procedure[a]

Case	Adaptive procedure				Uniform grid		
	N (final)	NGM	NI	NRRE	N	NI	NRRE
I	11	2	10	98	16	7	119
II	24	3	15	250	60	12	732
III	26	6	35	451	110	19	2109

[a] Values of N, NI and $\mathrm{NRRE} = (N+1)\mathrm{NI}$ to reach similar precision by employing a uniform grid are also given.

To evaluate the algorithm under more severe conditions, kinetic coefficients κ_{BD} and κ_{1Be} about ten times higher than those of Case I have been considered. Also, the H_2 saturation value $x_{H2,F}$ was increased by a factor close to four, what further increases the consumption rate of unsaturated species. A non-zero value for κ_{2Be} was assumed. The set of conditions is given in Table 3 (Case II). These kinetic parameters represent actual commercial catalysts more active than the sample of Case I.

The concentration profiles for Case II are plotted in Fig. 4. The effectiveness factor for BD is about 0.014. Half of the final 24 subintervals are located at $z > 0.85$, where BD and 1Be are sequentially depleted. Thus, the number of nodes needed to evaluate the consumption rate of BD and 1Be is similar as in Case I (Table 4). The adaptive procedure, by further shifting the nodes towards the external surface of the pellet, allows maintaining nearly the same number of nodes, in spite of higher consumption rates.

The additional nodes in Case II are employed for the hydrogenation of 2Be (ignored in Case I), which becomes depleted at nearly $z = 0.5$. The maximum in the 2Be profile arises because it is first formed near the surface from BD and 1Be and consumed in the interior of the pellet only when BD and 1Be have been depleted. Although, the average net production rate of 2Be is positive, its hydrogenation rate becomes greatly enhanced. Thus, the effectiveness factor for reaction 5 (Fig. 1) is 26.

Only one additional grid modification stage over those of Case I is needed (Table 4). The moderate increase in the overall number of iterations is essentially due to the additional grid modification stage.

The last case treated here (Case III in Table 3) is characterized by a relatively low value of κ_{BD}, a large adsorption constant K_{BD} and relatively large rate coefficients κ_{1Be} and κ_{2Be}. This case actually intends to represent the reaction of By (whose role is played by BD) in presence of 1Be and 2Be. The molar fraction profiles are depicted in Fig. 5. About three quarters of the 26 final subintervals (Table 4) are located at $z < 0.4$. This distribution reflects the fact that the fast 1Be and 2Be reactions can only take place once BD has been depleted. Six stages of grid modifications (NGM) were needed. The increase of NGM with respect to previous cases is in consequence of an unsuitable initial grid, $\{z_i\}_{i=0}^{i=7} = (0, 0.5, 0.7, 0.8, 0.9, 0.97, 0.99, 1)$. The number of overall iterations is again roughly proportional to NGM and the final number of subintervals is similar to that for Case II. It is interesting to note that 1Be reactions take place completely within the zone $0.2 < z < 0.3$. Also, within this zone the BD hydrogenation rate drops suddenly to zero and the 2Be hydrogenation rate reaches a maximum value. These changes can be better appreciated in Fig. 6, where the net consumption

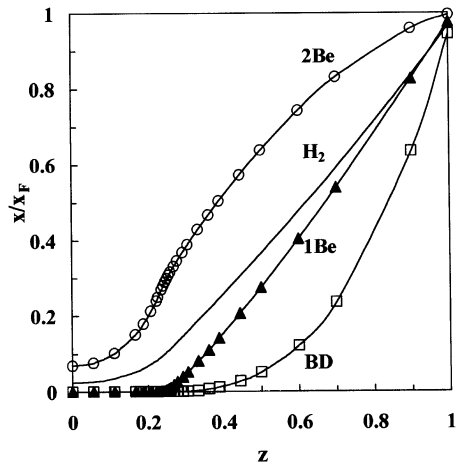

Fig. 5. Profiles for Case III (Table 2).

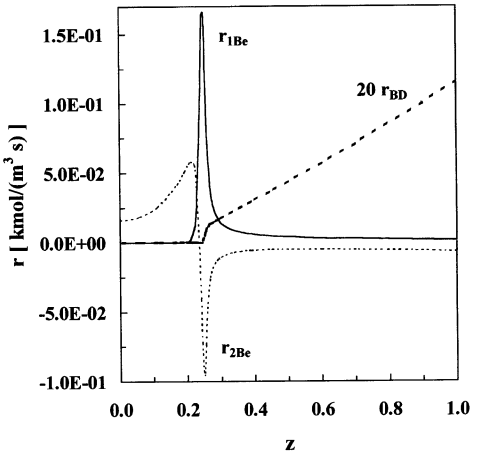

Fig. 6. Reaction rate profiles for Case III (Table 3).

rates of the three unsaturated species are plotted. Consequently, 12 out of the 26 subintervals correspond to that zone.

Case III is also useful to show that the coupling of reaction rates may difficult assessing in advance the behaviour of the system. The evaluation of Thiele moduli from the composition in the bulk fluid is practically meaningless in this case (all reactions are strongly inhibited by the level of BD concentration). Of course, a deeper analysis will eventually reveal the essential features. In this case, the Thiele modulus for BD reactions, $\Phi_{BD} = L\sqrt{r_{BD,F}/(C_T x_{BD,F} D_{HC})} = 3$, along with the fact that these reactions behave closely as being of zero order, allows to expect that BD will extinguish inside the pellet, giving place to the consumption of 1Be and 2Be. Considering for example reactions 3 and 4 for 1Be consumption (Fig. 1), a modified Thiele modulus can be evaluated from the fluid bulk composition, except for taking $x_{BD,F} = 0$. The value thus calculated, $\Phi_{3+4} = L\sqrt{(r_{3,F} + r_{4,F})/(C_T x_{1Be,F} D_{HC})} = 25$, suggests that 1Be will be consumed somewhere inside the pellet.

The three cases were also solved by employing equally spaced nodes. The initial guess values x_k° to start the iterations were evaluated as for the adaptive procedure. The number of subintervals given in Table 4 are those allowing a precision similar to that obtained by applying the adaptive procedure (about 10^{-4} in estimating $\overline{\mathbf{R}}$). The values of N and NRRE (also displayed in Table 4) are useful to compare both procedures. For the adaptive algorithm, NRRE is calculated by adding the contributions from all the stages in the procedure, $\mathrm{NRRE} = \Sigma_n(1 + N_n)\mathrm{NI}_n$, where n is the stage index. When employing equidistant nodes, $\mathrm{NRRE} = (N + 1)\mathrm{NI}$. NRRE is a direct indicator of the total computation task, as the evaluation of the reaction rate derivatives and operations for solving the linear system are also proportional to NRRE.

For the conditions at which the results in Table 4 were obtained, both N and NRRE provide similar conclusions. In Case I, the mildest case regarding diffusional limitations, the adaptive algorithm performs slightly better. Instead, in Cases II and III the adaptive algorithm shows a clear advantage over the use of equidistant nodes.

8. Conclusions

An integral formulation has been used as the basis of an h-adaptive algorithm for the evaluation of average reaction rates in catalytic reaction networks with strong diffusion limitations. The integrals are evaluated by employing local interpolating polynomials for the reaction rates.

The numerical solution scheme employed here was found to behave satisfactorily, as compared with FDs and other methods based on local cubic approximations. An additional advantage of the proposed numerical scheme, when using an adaptive mesh strategy is that any node introduces a single unknown, minimizing the impact of adding or eliminating nodes.

The adaptive mesh procedure is based on simple criteria applied on the estimation of the error resulting for the average reaction rates when a quadratic approximation is employed. Once a satisfactory grid is found, the final stage of the algorithm employs the cubic approximation.

The relevant formulation of the proposed algorithm comprises Eqs. (11a), (11b) and (11c) for the discretized equations, Eqs. (15a), (15b) and (15c) for the iterative solution according to Newton's linearization and the itemized criteria in Section 6 for the automatic adaptive mesh procedure.

The algorithm was tried for some cases corresponding to the catalytic hydrogenation of unsaturated C_4 compounds. Changes in reaction conditions leading to

a reduction of the effectiveness factor in about one order of magnitude demanded nearly the same number of nodes, displaced towards the catalyst surface, to deal with the fastest reactions. This result reveals the correct behaviour of the adaptive mesh procedure.

An example with a species showing the largest adsorption strength and a relatively low consumption rate (corresponding in practice to By) has been also presented. In this case, the fastest reactions demanding the highest concentration of nodes take place deeper inside the catalyst pellet. The adaptive mesh procedure also worked efficiently in this situation, as a suitable grid was reached in only six modification stages from an initial distribution strongly concentrated near the pellet surface.

It is concluded that the proposed algorithm is likely to perform efficiently and reliably for solving many problems of the class considered in this paper; i.e., multiple reaction systems with strong diffusion limitations, particularly when the location of fast reaction zones can not be known in advance. Instead, for problems with moderate Thiele moduli (properly defined), say $\Phi_k < 10$, the adaptive mesh procedure will loose significance and the use of a global method will usually be better. A similar conclusion applies, irrespective of the value of Φ, for most single reaction systems, since the penetration length can be estimated in advance.

The procedure here described for constant effective diffusivity can be extended to the treatment of more complex transport models. To this end, we are presently analyzing an approach based on the formulation outlined by Kaza and Jackson (1980) for the Dusty Gas Model. The system of equations is split into a second-order set of differential equations, formally equivalent to that considered here, and another set of first-order differential equations (defined by the transport model). There are reasons to expect that solving the sets alternately could result in an efficient iterative procedure to approach the global solution. If so, the algorithm here proposed can be used essentially as such for the second-order set, along with a standard procedure for the first-order set.

Acknowledgements

The authors wish to thank the support of the following argentine institutions: ANPCyT-SECyT (PICT No. 00227), CONICET (PIP96 No. 4791, Fellowship to NJM), UNLP (PID No. 11/I058, Fellowship to NOA). GDM, OMM and GFB are Research Members of CONICET, SPB is Professional Member of CIC (Bs.As.).

Appendix A

When linearizing the nodal values $\mathbf{r}_j$ for the Newton method, the effect of the increments $\Delta\mathbf{Y}_N$ through the stoichiometric relations (Eq. (13a)) were ignored (Eq. (14)), under the assumption of either large Biot numbers or similar ratios between them. Although, practical cases will usually justify this simplification, there are exceptions that will not. A typical example concerns thermal effects for reactions in gas phase. The thermal Biot number does not reach high values in these systems, and temperature increments are frequently larger outside than inside the pellet. In any case, we will present here a way to include the effect of $\Delta\mathbf{Y}_N$ with a minimum modification of the Newton linearized set of equation. The linearized nodal values should be written

$$\mathbf{r}_j = \mathbf{r}_j^{\circ} + \varphi_j \Delta\mathbf{Y}_j + (\partial\mathbf{r}/\partial\mathbf{Q})_j \sigma^* \Delta\mathbf{Y}_N. \tag{A1}$$

With these equations, the jacobian matrix will present, in comparison to that depicted in Eq. (18b), a full leftmost block column corresponding to the unknown $\Delta\mathbf{Y}_N$ in Eq. (A1). Direct gaussian elimination of this block column should not be done as this process would make non-zero blocks propagate below the main diagonal block of J, which in turn would have to be reduced (the number of additional operations required would be proportional to N^2). Instead, the following approach is suggested. We define a new vector variable $\mathfrak{I} = \sigma^* \Delta Y_N$. Then, Eq. (A1) becomes

$$\mathbf{r}_j = \mathbf{r}_j^{\circ} + \varphi_j \Delta\mathbf{Y}_j + (\partial\mathbf{r}/\partial\mathbf{Q})_j \mathfrak{I}. \tag{A2}$$

Including $\mathfrak{I}$ in the set of unknowns for the Newton iterations, the set of equations can be arranged as

$$\mathbf{J}\,[\Delta\mathbf{Y}_N, \Delta\mathbf{Y}_{N-1}, \mathbf{U}_{N-2}, \mathbf{H}_{N-2}, \Delta\mathbf{Y}_{N-2}, \ldots, \mathbf{U}_0, \mathbf{H}_0, \Delta\mathbf{Y}_0, \mathfrak{I}]^{\mathrm{T}} = -[\mathbf{d}_N^{\circ}, \mathbf{d}_{N-1}^{\circ}, \mathbf{0}, \mathbf{0}, \ldots, \mathbf{d}_0^{\circ}, \mathbf{0}]^{\mathrm{T}}, \tag{A3}$$

where the new matrix $\mathbf{J}$ is (for $N = 4$)

$$\mathbf{J} = \begin{array}{c|cccccccccccc}
 & \Delta\mathbf{Y}_4 & \Delta\mathbf{Y}_3 & \mathbf{U}_2 & \mathbf{H}_2 & \Delta\mathbf{Y}_2 & \mathbf{U}_1 & \mathbf{H}_1 & \Delta\mathbf{Y}_1 & \mathbf{U}_0 & \mathbf{H}_0 & \Delta\mathbf{Y}_0 & \mathfrak{I} \\
\hline
 & \alpha_4 & \beta_4 & \mathbf{I} & \mathbf{0} & & & & & & & \mathbf{0} & \gamma_4 \\
 & & \alpha_3 & -z_3\mathbf{I} & \mathbf{I} & \beta_3 & & & & & & -\mathbf{I} & \gamma_3 \\
 & & & \mathbf{I} & \mathbf{0} & -A_2\varphi_2 & -\mathbf{I} & & & & & \mathbf{0} & \varepsilon_2 \\
 & & & & \mathbf{I} & -B_2\varphi_2 & \mathbf{0} & -\mathbf{I} & & & & \mathbf{0} & \omega_2 \\
 & & & & & \alpha_2 & -z_2\mathbf{I} & \mathbf{I} & \beta_2 & & & -\mathbf{I} & \gamma_2 \\
 & & & & & & \mathbf{I} & \mathbf{0} & -A_1\varphi_1 & -\mathbf{I} & & \mathbf{0} & \varepsilon_1 \\
 & & & & & & & \mathbf{I} & -B_1\varphi_1 & \mathbf{0} & -\mathbf{I} & \mathbf{0} & \omega_1 \\
 & & & & & & & & \alpha_1 & -z_1\mathbf{I} & \mathbf{I} & \beta_1-\mathbf{I} & \gamma_1 \\
 & & & & & & & & & \mathbf{I} & \mathbf{0} & -A_0\varphi_0 & \varepsilon_0 \\
 & & & & & & & & & & \mathbf{I} & -B_0\varphi_0 & \omega_0 \\
 & \alpha_0 & \beta_0 & -\mathbf{I} & \mathbf{I} & & & & & & & -\mathbf{I} & \gamma_0 \\
 & \sigma^* & \mathbf{0} & \mathbf{0} & \mathbf{0} & & & & & & & & -\mathbf{I}
\end{array} \tag{A4}$$

with

$$\gamma_N = a_{N,N}(\partial\mathbf{r}/\partial\mathbf{Q})_N + a_{N,N-1}(\partial\mathbf{r}/\partial\mathbf{Q})_{N-1},$$

$$\gamma_i = (b_{i,i} - z_i a_{i,i})(\partial\mathbf{r}/\partial\mathbf{Q})_i + (b_{i,i-1} - z_i a_{i,i-1})(\partial\mathbf{r}/\partial\mathbf{Q})_{i-1} \quad (i = 1, \ldots, N-1),$$

$$\gamma_0 = (b_{N,N} - a_{N,N})(\partial\mathbf{r}/\partial\mathbf{Q})_N + (b_{N,N-1} - a_{N,N-1})(\partial\mathbf{r}/\partial\mathbf{Q})_{N-1},$$

$$\varepsilon_i = -A_i(\partial\mathbf{r}/\partial\mathbf{Q})_i,$$

$$\omega_i = -B_i(\partial \mathbf{r}/\partial \mathbf{Q})_i \quad (i = 0,\ldots, N-2,)$$

To solve Eq. (A3), the reduction of the new bottom blocks and the treatment of the new rightmost block column of J involve a number of additional operations proportional to N.

References

Abashar, M. E., & Elnashaie, S. S. (1993). Mathematical modelling of diffusion–reaction, and solution algorithm for complex reaction networks in porous catalyst pellets-steam reforming of natural gas. *Mathematical Computational Modelling*, *18*, 85–100.

Boitiaux, J.P., Cosyns J., Derrien M., Leger G. (1985). Newest hydrogenation catalysts. Hydrocarbon Processing, 51–59.

Bressa, S. P., Ardiaca, N. O., Martinez, O. M., & Barreto, G. F. (1998). Analysis of operating variables in the catalytic purification of 1-butene in trickle bed reactors. *Chinese Journal of Chemical Engineering*, *6*(2), 103–115.

Giona, M., & Baratti, R. (1993). Fixed point method in steady state analysis application to catalyst pellets. *Chemical Engineering and Communication*, *122*, 57–67.

Gonzo, E. E., Gottifredi, J. C., & Romero, L. C. (1998). Effectiveness factors and selectivity for parallel catalytic reactions with Langmuir-Hinshelwood kinetics. *Chemical Engineering Science*, *43*, 1410–1413.

Gottifredi, J. C., Gonzo, E. E., & Froment, G. F. (1994). Diffusion and reaction inside a catalyst pellet for a parallel-consecutive reaction scheme. *Chemical Engineering Science*, *49*, 2399–2403.

Golberg, M. A., Chen, C. S., & Bowman, H. (1999). Some recent results and proposals for the use of radial basis functions in the BEM. *Engineering Analysis in Boundary Elements*, *23*, 185–296.

Kaza, K. R., & Jackson, R. (1980). Diffusion and reaction of multicomponent gas mixtures in isothermal porous catalysts. *Chemical Engineering Science*, *35*, 1179–1187.

Kaza, K. R., Villadsen, J., & Jackson, R. (1980). Intraparticle diffusion effects in the methanation reaction. *Chemical Engineering Science*, *35*, 17–24.

Krishsna, R., & Sie, S. T. (1994). Strategies for multiphase reactor selection. *Chemical Engineering Science*, *49*, 4029–4065.

Press, W. H., Teukolsky, S. A., Vetterling, W. T., & Flannery, B. P. (1992). *Numerical recipes*. Cambridge: Cambridge University Press.

Ramachandran, P. A. (1994). *Boundary element method in transport phenomena*. Southampton: Computational Mechanical Publications.

Schilson, R. E., & Amundson, N. R. (1961). Intraparticle diffusion and conduction in porous catalysts-II complex reactions. *Chemical Engineering Science*, *13*, 237–244.

Villadsen, J., & Michelsen, M. L. (1978). *Solution of differential equations models by polynomial approximation*. New Jersey: Prentice Hall.

Weinberger, H. F. (1967). *Partial differential equations*. New York: Blaisdell Publishing.

Wendt, J. O. L., Martinez, C. H., Lilley, D. G., & Corley, T. L. (1979). Numerical solution of stiff boundary valued problems in kinetics and diffusion. *Chemical Engineering Science*, *34*, 527–537.

Wohlfahrt, K., & Hofmann, U. (1979). Concentration and temperature profiles for complex reactions in porous catalysts. *Chemical Engineering Science*, *34*, 491–501.